Electronic Supplementary Material (ESI) for Journal of Materials Chemistry C.

Supporting Information

Neural Network Design of Broadband Epsilon Near Zero Perfect Optical Absorbers

David Dang[1], Aleksei Anopchenko[1], Sudip Gurung[1], Zoey Liu[1], Xuguo Zhou[1], and Ho Wai Howard Lee[1*]

[1] Department of Physics & Astronomy, University of California, 4129 Frederick Reines Hall, Irvine, CA 92697, United States

[*]Corresponding author: howardhw.lee@uci.edu

Supplementary Section 1: Neural Network Training

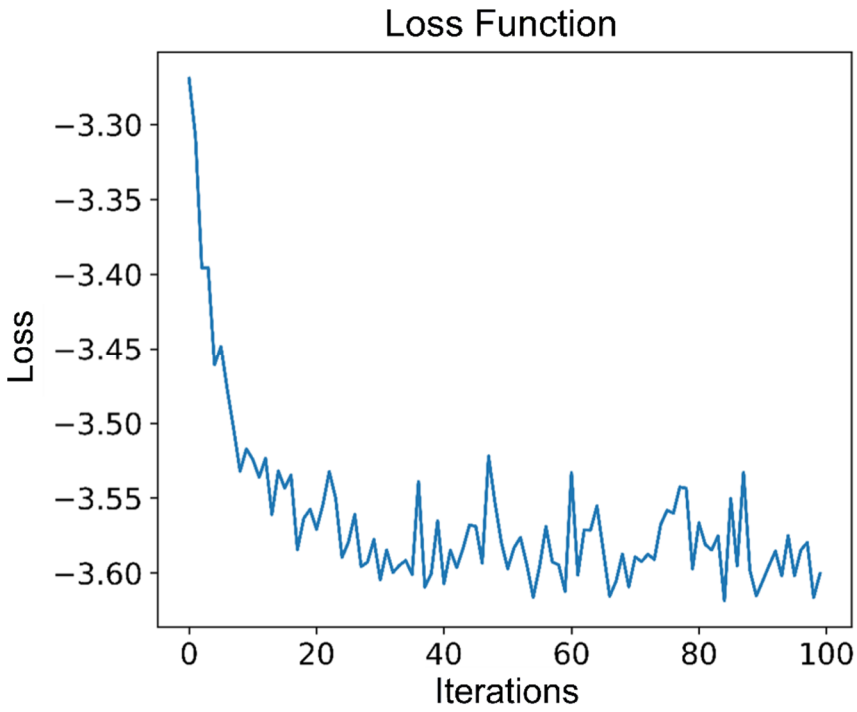

Figure S1 Loss Function for 10 Layers: Training performance of the neural network via observation of the loss function versus number of batch (or iterations). Lower values indicate better performance.

As discussed in the main manuscript, we employed a residual generative nerual network that was made up residual neural network blocks. We employed a relatively deep and wide neural network architecture by using 12 of the neural network blocks. Each neural network block had the following layers: input layer (512 neurons), fully connected layer (1024 neurons), batchnormalization, leaky ReLU (hyperparameter of 0.2), fully connected layer (1024 neurons), fully connected layer (512), and a resiudal layer with a leaky ReLU (hyperparameter of 0.2). Despite the large number of layers, the neural network converges in a reasonable number of iterations. As shown in Figure S6, the loss function reaches a horizontal plateau near 40 iterations. Each iteration used a batch size of 10, where the loss and gradients of 10 thin films stacks are averaged for backpropgation for mini batch gradient descent.

Supplementary Section 2: Optical Properties of Thin Film Stack.

The dielectric function of the indium tin oxide layer ε_{ITO} can be described by the Drude model:

$$\varepsilon_{ITO}(\omega) = \varepsilon_{\infty} - \frac{\omega_p^2}{\omega^2 + i\omega\Gamma} \quad \text{where} \quad \omega_p = \sqrt{\frac{Ne^2}{\varepsilon_0 m^*}} \text{ and } \Gamma = \frac{e}{\mu \cdot m^*}$$

The neural network designed 10-layer stack was optimized by changing the carrier densities in the Drude model and varying the thicknesses, which is shown in Table S1. All other parameters, such as effective mass, electron collision rate and epsilon infinity, in the Drude model were kept constant and are shown in Table S2. The refractive index and extinction coefficients as well as the real and imaginary parts of complex permittivity for the entire thin film stack is shown in Figure S1 and S2, respectively.

Table S1: Electron Density, Thickness, and Plasma Frequency of ITO Layers for Neural Network Designed Thin Film Stack

Nth ITO Layer	Electron Density (10^{20} cm^{-3})	Thickness (nm)	Plasma Frequency ω_p (10^{15} $rad \cdot s^{-1}$)	ENZ Wavelength (nm)	Imaginary Permittivity at ENZ Wavelength
1	6	10	2.61	1515	1.41
2	5	10	2.38	1682	1.56
3	12	9	3.69	1038	0.96
4	8.5	9	3.11	1247	1.16
5	5	9.8	2.38	1682	1.56
6	18	6	4.52	839	0.78
7	20	9	4.77	795	0.74
8	6	5	2.61	1515	1.41

Table S2: Fixed Drude Model Parameters for ITO Layers

Constant Drude Model Parameters	
Permittivity at high-frequency limit, ε_{∞}	3.9
Mobility μ ($cm^2 \cdot V^{-1} \cdot s^{-1}$)	14
Effective Mass	0.28 x m_e
Collision rate, Γ ($rad \cdot s^{-1}$)	0.449 x 10^{15}

Table S3: Subwavelength Thicknesses

Number of ITO Layers	Maximum Wavelength of Absorption (λ)	Total Thickness of ITO Layers (D)	Deep Subwavelength Thickness (λ/D)
5	956	24	39.8
6	1161	36	32.2
7	1173	45.5	25.8
8	1250	51	24.5
9	1245	64	19.5
10	1438	67.8	21.2
11	1455	76	19.1
12	1455	88.9	16.4

To ensure that the subwavelength thickness was not artificially decreased by the carrier density range initially chosen, we extended the maximum wavelength range from 2000 nm to 3000 nm and changed the carrier density from 1×10^{20} cm^{-3} to 20×10^{20} cm^{-3} in 1×10^{19} cm^{-3} steps. We then trained on 1000 12-layer devices and generated 10000 12-layer stacks. By averaging the subwavelength thicknesses of the top 100 broadband devices, we found that the average subwavelength thicknesses of our 12-layer stack is 16.03 which is more or less the same as the subwavelength thicknesses reported in Table S3 despite extending the range of parameters.

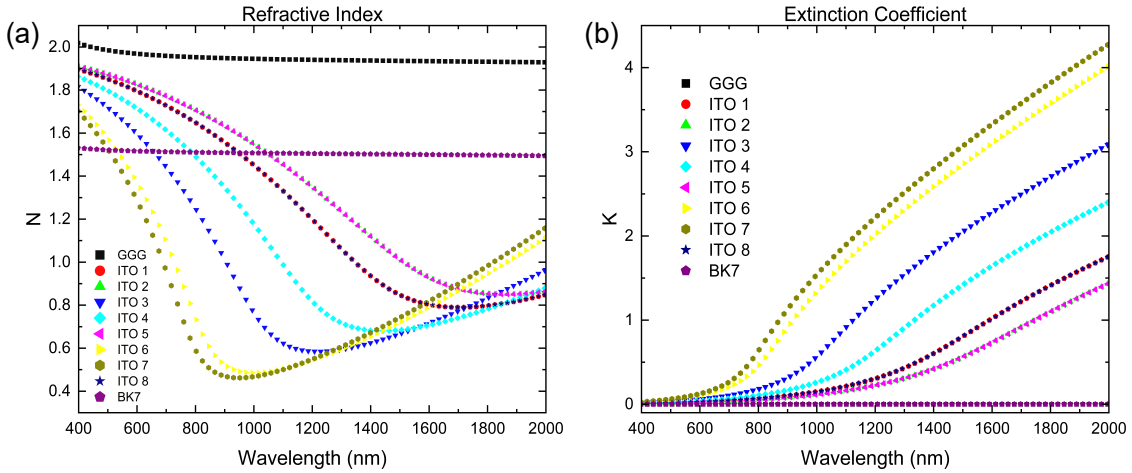

Figure S2: Refractive Index and Extinction Coefficient n (a) and k (b) values for all 10 layers of the neural network designed absorber. ITO 1 and ITO 8 as well as ITO 1 and ITO 5 have the same optical properties, respectively.

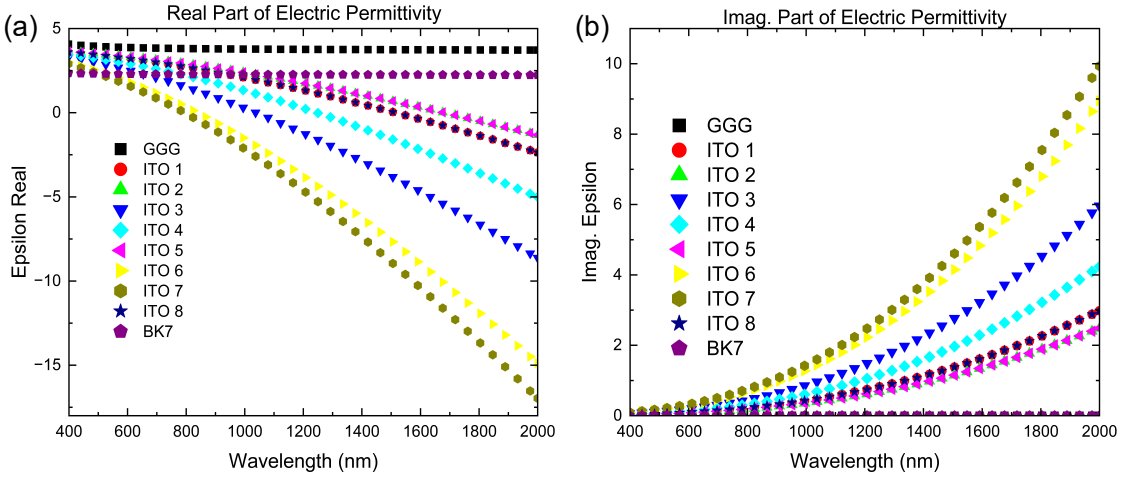

Figure S3: Real (a) and imaginary (b) part of the electric permittivity for all 10 layers of the neural network designed absorber.

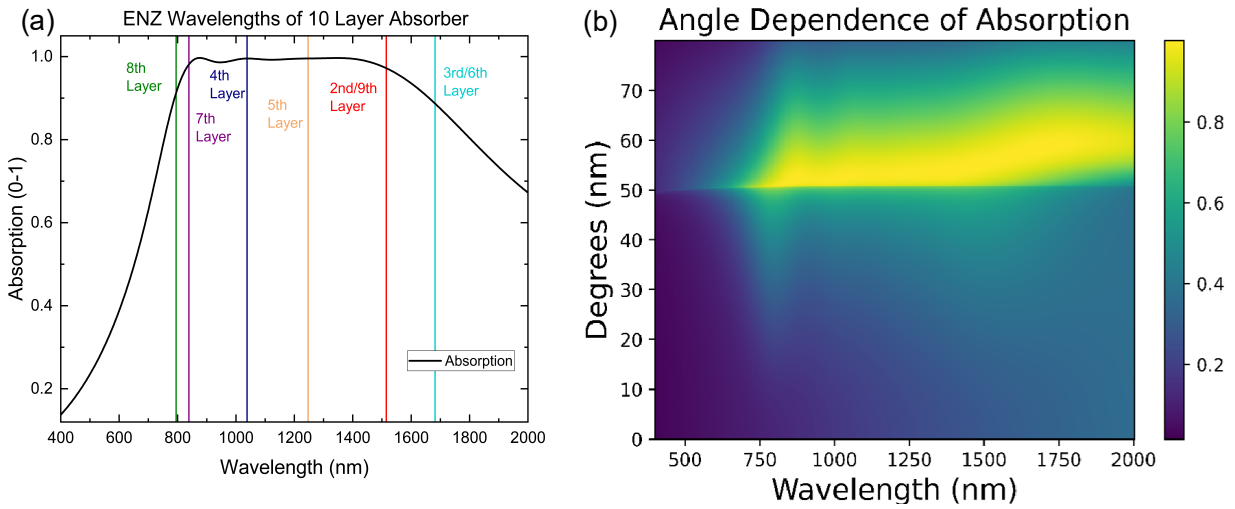

Figure S4: ENZ Wavelength Profile. (a) Corresponding ENZ wavelengths for each layer of the neural network designed 10-layer stack.(b) Simulation of the absorption spectrum for the neural network designed 10-layer stack at multiple angles.

In Figure S4a, we plot the the ENZ wavelengths of the stack (see the Table S1) as well as the absorption profile of our thin film. The position of the ENZ wavelengths suggest intelligent design by the neural network- the neural network has learned how to arrange the ENZ wavelengths in such a manner to achieve broadband perfect absorption. The absorption spectra of Figure S4b shows that our neural network designed broadband absorber is slightly broad in angle, with bandwidth of approximatively 8 degrees.

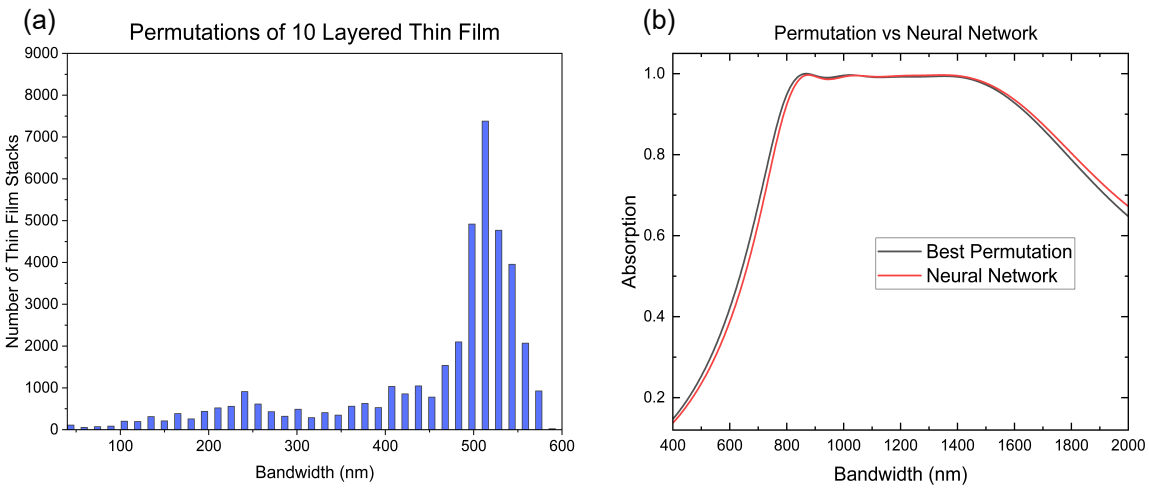

Figure S5: Permutation of all ordered layers vs Neural Network. (a) Histogram displaying the bandwidth of thin film stacks generated by performing a permutation of all the layers of the best performing neural network designed 10-layer thin film. (b) Comparison of the absorption spectra of neural network design verse the best permutation (519.8 nm for neural network compared to 588 nm for permutation).

To gauge how effective our neural network is at choosing the most optimal order layer, we performed a physics simulation for all permutations of the ITO layers for our 10-layer film. The order of the ITO layers was shuffled around. As shown by Figure S5a and Figure S5b, the total number of permutations equaled 40,320 or 8!, achieving a median bandwidth of 455 nm and a maximum bandwidth of 588 nm. Although our original neural network design did not have the best possible order of materials, it was able to find a near optimal order of layers. Overall, this is still an impressive feat by the neural network considering during generation we only sampled 1000 films. In other words, if we consider the total design spaced consisted of billions of combinations of thicknesses as well as carrier densities- the neural network achieved 13% less bandwidth than the most optimal permutation while only sampling an extremely tiny fraction of the design space.

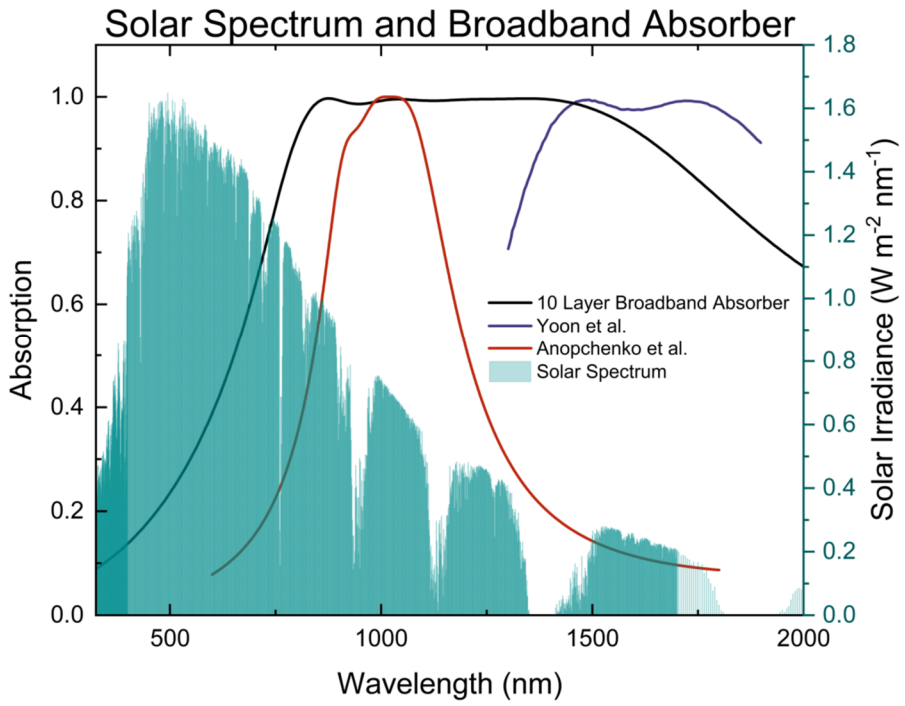

Figure S6: Comparison of Broadband Absorbers in Literature verse Solar Spectrum: Absorption spectra of different ITO broadband absorbers under 150 nm thickness reported in literature[1, 2]. The broadband absorber reaches into the near infrared- a region of solar energy usually wasted by conventional silicon based solar cells[3].

The large perfect absorption bandwidth in the near infrared opens the possibilities for more efficient solar cells. Conventional silicon based solar cells typically absorb light in a region from approximately 300 to 1100 nm[4], and as a result, the solar energy beyond 1100 nm is often wasted or inaccessible. Our ENZ thin film stack as aforementioned performs optimally in the region above 1100 nm (Figure S6), and hence could potentially be integrated into a photovoltaic cell to capture a wider range of the solar spectrum[5, 6].

Supplementary Section 3: Technical Performance of TMM Fast

The following information is a performance review of the TMM Fast[7] - an extremely fast implementation of the Abeles transfer matrix method for thin film stacks, originally written in python by Steven J Byrnes. This implementation was developed by Alexander Luce in collaboration with Heribert Wankerl at Osram.

TMM Fast comes in two variations that were examined in this work: CPU only and GPU acceleration. We examined the algorithms performance by calculating the transmission spectra with 1000, 10-layer thin film stack and constant n and k values of 1 and 0 respectively from 0 to 60 degrees in 5-degree steps and from wavelengths of 400 nm to 2000 nm with 4 nm steps. The program was run on a 12th generation Intel Core i5-12600K with a RTX 3090 GPU and the computation time was calculated with the "timeit" magic function; timeit measures the computation time of an algorithm by repeating the algorithm seven times and then averaging as well as finding the standard deviation of the recorded time to complete. With CPU only, our algorithm ran in 7.27 s ± 55.6 ms per loop, while the GPU variant ran significantly faster with 631 ms ± 1.57 ms per loop. As a result, GPU acceleration is an order of magnitude faster than performing the calculations on a CPU.

References:

1. A. Anopchenko, L. Tao, C. Arndt and H. W. H. Lee, *ACS Photonics*, 2018, **5**, 2631-2637.
2. J. Yoon, M. Zhou, M. Badsha, T. Y. Kim, Y. C. Jun and C. K. Hwangbo, *Scientific Reports*, 2015, **5**, 1-8.
3. C. A. Gueymard, D. Myers and K. Emery, *Solar energy*, 2002, **73**, 443-467.
4. H. Ahmed, S. McCormack and J. Doran, *International Journal of Spectroscopy*, 2016, **2016**.
5. G. Conibeer, *Materials today*, 2007, **10**, 42-50.
6. M. A. Green, *Physica E: Low-dimensional Systems and Nanostructures*, 2002, **14**, 65-70.
7. A. Luce, A. Mahdavi, F. Marquardt and H. Wankerl, *JOSA A*, 2022, **39**, 1007-1013.